Dielectric Properties and 3D Printing Fesibility of UV Curable Polymer Composites

Conference Paper · September 2018

DOI: 10.1109/ICHVE.2018.8642258

6 authors, including:

Wendong Li
Xi'an Jiaotong University
40 PUBLICATIONS **341** CITATIONS
SEE PROFILE

Liyuan Zhang
Xi'an Jiaotong University
6 PUBLICATIONS **43** CITATIONS
SEE PROFILE

Chao Wang
xjtu
20 PUBLICATIONS **121** CITATIONS
SEE PROFILE

Li Xiaoran
Xi'an Jiaotong University
19 PUBLICATIONS **125** CITATIONS
SEE PROFILE

Dielectric Properties and 3D Printing Fesibility of UV Curable Polymer Composites

Wen-Dong Li, Li-Yuan Zhang, Chao Wang, Xiao-Ran Li, Man Xu, Guan-Jun Zhang*
State Key Laboratory of Electrical Insulation and Power Equipment, Xi'an Jiaotong University
Xi'an, Shaanxi 710049, China
*gjzhang@xjtu.edu.cn

***Abstract*: In this study, UV curable polymer composites are investigated to explore their applicability in building the dielectrics with functionally graded material (d-FGM) using stereolithographic 3D printing technology. On the prepared test samples, several dielectric properties, i.e., permittivity, dielectric loss and breakdown strength, are characterized. 3D printing feasibility of the polymer composites are also investigated by measuring the viscosity and curing depth. Finally, influences of the ceramic filler's type, volume fraction and particle morphology on the dielectric properties and 3D printing feasibility are discussed.**

Keywords—Functionally graded material; Polymer Composites; UV Curable Resin; Dielectric Properties; 3D Printing.

I. INTRODUCTION

Dielectrics with functionally graded materials (d-FGM) are materials with spatially non-uniform dielectric properties, i.e., permittivity ε and conductivity σ. By using d-FGM, the E-field distribution of solid insulators could be effectively improved without complicating the geometry. Although the effectiveness of d-FGM on E-field improvement has been extensively verified [1, 2], the implementation of d-FGM is still a challenging project due to the lack of flexible and precise fabrication methods.

3D printing, as an additive manufacturing approach, could be a solution for the challenge of d-FGM fabrication. In 3D printing processes, the materials are successively accumulated to build three dimensional objects. Therefore, if the permittivity ε or conductivity σ of the building material could be precisely adjusted during the accumulating process, the fabrication of d-FGM will be realized [3]. So far, there are many different technologies in 3D printing, such as stereolithography (SLA), selective laser sintering (SLS) and fused deposit modeling (FDM). Among these, SLA method has a higher accuracy and can fabricate objects without internal air bubbles [4], which means it would be more suitable for fabrication of insulation materials.

To build d-FGM insulator with 3D printing, a permittivity or conductivity adjustable material is required. This is usually done by the mixing two kind of materials while one has low ε or σ and another one has high ε or σ. The former material is usually polymers and the latter is usually ceramic or carbon materials. Kurimoto et al. and our group [5, 6] added TiO_2 (ε_r=114) or $BaTiO_3$ (ε_r>2000) fillers with epoxy resin (ε_r=3.5) to adjust the relative permittivity ε_r in the range from 4 to 12. Similar approach could be applied to the 3D printing materials such as UV curable resin used in SLA method. However, improper particle size, shape and volume fraction might deteriorate resin fluidity and UV light transmittance, and further cause failure to the SLA process.

In this paper, UV curable polymer composites are investigated to explore their applicability in d-FGM and SLA 3D printing technique. During the sample preparation, a molding technique is applied to improve the reproducibility. Volume fraction and particle size of the fillers' are controlled. Finally, influences of the filler's type, volume fraction and particle morphology on the dielectric properties, as well as 3D printing related properties (viscosity and curing depth), are discussed to give insights on building the material system.

II. EXPERIMENTAL SETUP

A. Materials

The HighTemp (HT) resin form Formlabs Inc. (United States) was used as the matrix material. We choose this resin due to its good heat resistance. According to [7], the highest heat deformation temperature (HDT) of High Temp resin is 289 °C, which indicates good thermal stability. The ceramic fillers used in this study include alumina (Al_2O_3), strontium titanate ($SrTiO_3$) and barium titanate ($BaTiO_3$), whose physical properties are shown in Table I. Obviously, these fillers could be categorized into small size fillers and large size ones. The D_{50} of large size fillers is about 10 times larger than the small ones. The alumina fillers were from Bestry Performance Materials Co., Ltd. (Shanghai, China) and have a spherical shape. Small size $SrTiO_3$ and $BaTiO_3$ were from Aladdin (Shanghai, China), and large size $SrTiO_3$ and $BaTiO_3$ were from Dian Yang Industrial Co., Ltd. (Shanghai, China). All the ceramic fillers were used as received.

TABLE I. PROPERTIES OF THE CERAMIC FILLERS

Filler Type	Average Particle Size D_{50} (μm)	True Density (g/cm^3)	ε_r
Small size Al_2O_3	2.17	3.85	10
Small size $SrTiO_3$	3.71	5.04	300
Small size $BaTiO_3$	3.27	5.98	3000
Large size Al_2O_3	31.07	3.85	10
Large size $SrTiO_3$	32.58	4.94	300
Large size $BaTiO_3$	32.09	5.59	3000

This work was supported by the National Natural Science Foundation of China (U1766218) and by National Basic Research Program of China (973 Program) (2015CB251003)
978-1-5386-5086-8/18/$31.00 ©2018 IEEE

B. *Sample Preparation*

The ceramic fillers were dried at 100°C in vacuum for 8h, then were mechanically mixed and stirred with HT resin for 3h. The stirring procedure was conducted in vacuum to remove air bubbles inside the suspension. Finally, bubble-free resin suspensions with different filler's volume fraction V_f were prepared, as shown in Table II.

TABLE II. SAMPLES USED IN THIS STUDY

Sample Name	Resin Type	Filler Type	V_f/%
Pure Resin	HighTemp	--	0
HT/AL-S	HighTemp	Small size Al_2O_3	5~20
HT/AL-L	HighTemp	Large size Al_2O_3	
HT/ST-S	HighTemp	Small size $SrTiO_3$	
HT/ST-L	HighTemp	Large size $SrTiO_3$	
HT/BT-S	HighTemp	Small size $BaTiO_3$	
HT/BT-L	HighTemp	Large size $BaTiO_3$	

The test samples were prepared using an molding method described in Figure 1, which includes, a) preparation of the silicone rubber mold, b) injection of resin suspension into the mold, c) covering the mold with a quartz cover pasted with polyethylene terephthalate (PET) film, and d) UV curing of the suspension in a customized curing box, in which a 405nm LED array are applied as the UV source. The radiation power was adjusted to 30 mW/cm^2 and curing time set to 120 min. The curing temperature was set to 60°C according to the recommendation of resin manufacturer. Afterwards, the test samples were obtained, which have a smooth surface and good geometric accuracy for the characterization.

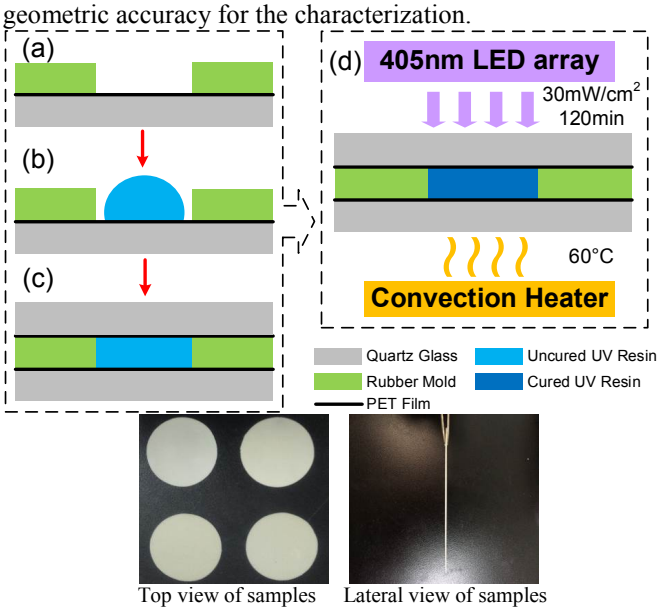

Figure 1. Description of the molding method

C. *Characterization*

Scanning electron microscopy was used to examine the cross-sectional microstructure of resin composites. Before SEM observation, test samples were sputtered with gold to avoid surface charging. For the dielectric properties, relative permittivity, dielectric loss and breakdown strength of the test samples were investigated. A Tettex 2821 Schering bridge was used to measure the relative permittivity and dielectric loss under AC voltage (50Hz). The breakdown strength under 50Hz AC were also measured according to IEC 60243 standard. Sphere-sphere electrode system with 25mm diameter was applied. The electrodes were immersed in mineral oil to prevent surface flashover.

The material properties related to SLA process were also characterized, including the viscosity and UV curing depth. The viscosity of uncured resin composites were measured by a NDJ-79A rotary viscometer. By immersing the test chamber inside a thermostatic water bath, temperature was controlled to be constant during viscosity measurement. For the UV curing test, the uncured composite resin was put under 405nm UV exposure for specific UV light energy. The cured resin sheets were cleansed with isopropanol and their thickness were measured using a thickness gauge with 0.001mm accuracy.

III. RESULTS

A. *Microstructure of UV cured composites*

Figure 2 illustrates the microstructure of the resin composites according to SEM observation. It is shown that all the large size fillers have spherical particle shape. For the small size fillers, the Al_2O_3 filler is spherical while the $BaTiO_3$ and $SrTiO_3$ fillers are irregular in shape. Moreover, the fillers with small size and irregular shape (Figure 2e-f) have a higher probability of agglomeration. This phenomenon could be caused by the effects of particles' size and shape on their specific surface area, i.e. large and spherical fillers would have less specific surface area than small and irregular fillers. Hence, fillers with larger size and spherical shape would have better dispersion inside the composite materials.

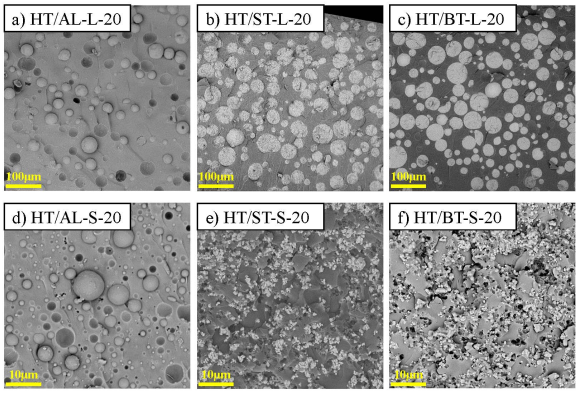

Figure 2. Cross-sectional SEM images of test samples with 20vol% filler loading

B. *Dielectric Properties*

Figure 3 illustrates the permittivity ε_r of composite materials. In general, increasing of filler concentration can lead to higher permittivity value. When the ceramic fillers is loaded at 20vol%, the ε_r of HT/BT and HT/ST composites will increase to 6~8, which is about 1.5~2 times higher than that of pure resin and HT/AL. However, the difference of permittivity

between HT/BT and HT/ST samples are not very significant. The filler size also have some influences on the permittivity results. In most cases shown in Figure 3, composites with small size fillers have higher permittivity than that with large size fillers. This can be caused by the interfacial polarization between resin matrix and ceramic fillers. The specific surface area of small size fillers is higher than large size fillers. Therefore, more interfacial area would be introduced when loaded with small size fillers, which would further lead to stronger interfacial polarization and increase the permittivity of composite materials.

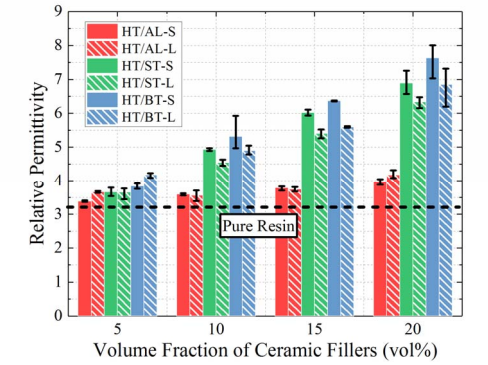

Figure 3. Dielectric permittivity of UV resin composites

Figure 4 depicts the dielectric loss of the UV resin composites. It can be seen that the dielectric loss of cured pure HT resin is about 0.006, which is similar to the epoxy material [8]. For most cases of the composite resin, the HT/ST and HT/BT composites have higher tanδ than HT/AL composites, which can be attributed to the special properties of SrTiO3 and BaTiO3 materials. In other words, the electric hysteresis nature of these ferroelectric materials would cause more energy loss under AC voltage excitation.

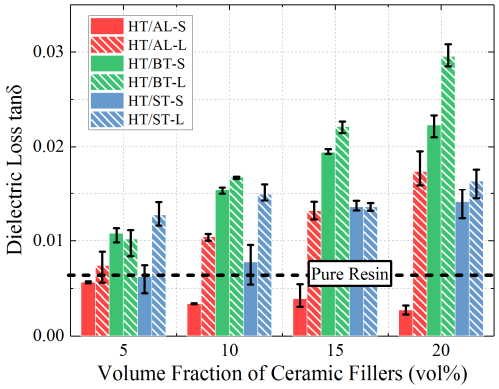

Figure 4. Dielectric loss of the UV resin composites

Figure 5a illustrates the dielectric strength E_b of the resin composites. With the increase of filler concentration, the E_b of HT/ST and HT/BT composites are decreased, while E_b of HT/AL composites remain almost constant. This might be caused by the difference of electric field distribution in the breakdown test system. As in Figure 5b, with the increase of sample's permittivity, the E-field strength in the oil gap is significantly increased, which will lead to breakdown of the oil gap and further causes bulk breakdown of test samples [9]. Therefore, it seems that DC breakdown test is more suitable for the solid samples with variable permittivity values.

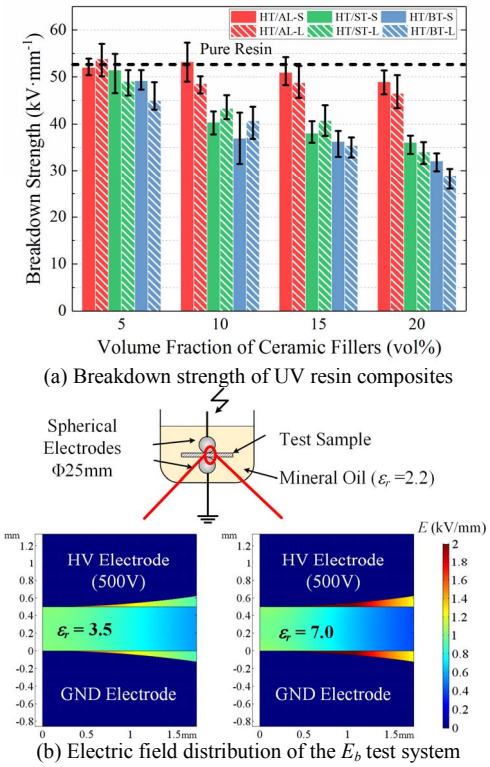

Figure 5. Electric breakdown test of the UV resin composites

C. 3D printing related material properties

Figure 6 illustrates the viscosity test results of uncured composite resin at 30°C. Obviously, higher filler concentration will lead to increased viscosity. Compared to the HT/ST and HT/BT resins, the HT/AL resin has much lower viscosity, which means the fluidity of HT/AL composites are superior to HT/BT and HT/ST composites. This can be attributed to the difference of filler's surface morphology. According to [10], spherical fillers with smooth particle surface, which is the case for Al_2O_3 fillers, will facile the resin flow around the filler's interfacial area and reduce the viscosity of the suspension.

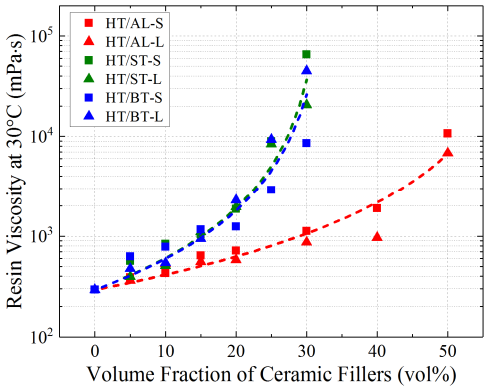

Figure 6. Viscosity of uncured resin composites

Figure 7 illustrates the curing depth of resin composites with variable UV exposure energy. From Figure 7a, it is indicated that introducing ceramic fillers into the resin will reduce the curing depth. Besides, the curing depth of HT/AL resin is much higher than that of HT/BT and HT/ST samples. Moreover, the composites with large size fillers have higher curing depth than the small size fillers. These phenomena can be caused by the particle scattering of UV lights. According to [11], the light scattering by solid particles is affected by the refractive index n and size of filler particles. Lower n and larger particle size could reduce the light scattering and increase the curing depth of UV resin.

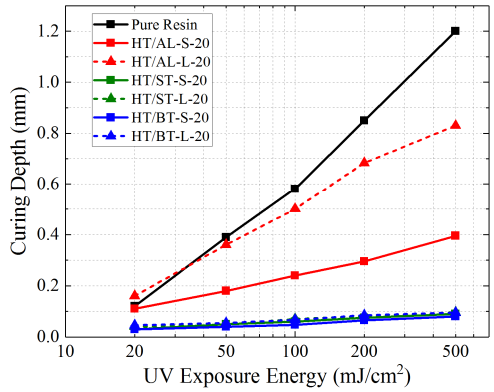

(a) composite samples with 20vol% filler loading

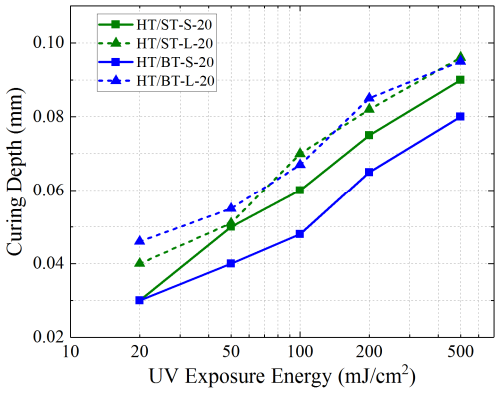

(b) HT/ST and HT/BT samples with 20vol% filler loading

Figure 7. Curing depth of the resin samples

For the SLA technique in this study, the thickness of one resin layer is 25~100 μm. To improve the mechanical strength of the resin layer, the curing depth should be at least higher than 50 μm. According to Figure 7b, at least 100 mJ/cm^2 of UV exposure is required, which could be realized by reducing the laser scan speed of the 3D printer [12].

IV. CONCLUSIONS

a) All the studied properties are influenced by the volume fraction of the fillers. In general, higher filler loading will lead to the increase of permittivity, but might also increase the dielectric loss. In addition, high filler loading may also hinder the printability of the resin composites, by decreasing the fluidity and curing depth.

b) The filler type will also affect these material properties. For instance, by choosing ceramic fillers with high permittivity value (e.g. $SrTiO_3$ and $BaTiO_3$), the permittivity of the composites will be significantly increased, whereas the UV curing depth will be decreased which bring difficulty to the 3D printing process.

c) The particle morphology of ceramic fillers is important for the 3D printing feasibility, though it may not have significant correlation with the dielectric properties. It seems that fillers with spherical shape, smooth surface and relatively large particle size will facile the 3D printing process.

In s, it could be concluded that the filler properties has strong influences on these material properties. In order to give out practical suggestions on the material system of 3D printable FGM insulation, The underlying mechanisms of these influences will be studied in future.

REFERENCES

[1] M. Kurimoto, K. Kato, M. Hanai, Y. Hoshina, M. Takei, and H. Okubo, "Application of Functionally Graded Material for Reducing Electric Field on Electrode and Spacer Interface", IEEE Transactions on Dielectrics and Electrical Insulation, Vol. 17, No. 1, pp. 256-263, 2010.

[2] W. D. Li, X. Y. You, H. B. Mu, J. B. Deng, and G. J. Zhang, "Numerical optimization and 3D-printing fabrication concept of high voltage FGM insulator", IEEE PES Asia-Pacific Power and Energy Engineering Conference (APPEEC), Brisbane, QLD Australia, 2015, pp. 1-4.

[3] Z. Liu, W.-D. Li, Y.-B. Wang, G.-Q. Su, Y. Cao, G.-J. Zhang, and D.-C. Li, "Topology Optimization and 3D-Printing Fabrication Feasibility of High Voltage FGM Insulator", IEEE International Conference on High Voltage Engineering and Application (ICHVE 2016), Chengdu, China, 2016, pp. 1-4.

[4] M. Kurimoto, H. Ozaki, Y. Yamashita, T. Funabashi, T. Kato, and Y. Suzuoki, "Dielectric Properties and 3D Printing of UV-cured Acrylic Composite with Alumina Microfiller", IEEE Transactions on Dielectrics and Electrical Insulation, Vol. 23, No. 5, pp. 2985-2992, 2016.

[5] H. Ozaki, M. Kurimoto, T. Sawada, T. Funabashi, T. Kato, and Y. Suzuoki, "Evaluation of relative permittivity and coefficient of thermal expansion of TiO_2/SiO_2 epoxy composites for permittivity-graded insulator", 2017 IEEE Conference on Electrical Insulation and Dielectric Phenomenon (CEIDP), 2017, pp. 568-571.

[6] L. Y. Zhang, M. Xu, W. D. Li, Z. Liu, and G. J. Zhang, "Fabrication and characterization of BaTiO3/Al2O3/epoxy composites with tunable dielectric permittivity", 2016 IEEE International Conference on High Voltage Engineering and Application (ICHVE), 2016, pp. 1-4.

[7] Formlabs_Inc., Datasheet of HighTemp Resin, 2016.

[8] P. Luo, M. Xu, S. Wang, and Y. Xu, "Structural, dynamic mechanical and dielectric properties of mesoporous silica/epoxy resin nanocomposites", IEEE Transactions on Dielectrics and Electrical Insulation, Vol. 24, No. 3, pp. 1685-1697, 2017.

[9] J. Kuffel, E. Kuffel, and W. S. Zaengl, High voltage engineering fundamentals, Oxford: Newnes, 2000.

[10] S. Mueller, E. W. Llewellin, and H. M. Mader, "The rheology of suspensions of solid particles", Proceedings of the Royal Society a-Mathematical Physical and Engineering Sciences, Vol. 466, No. 2116, pp. 1201-1228, 2010.

[11] Y. Yang, Z. Chen, X. Song, B. Zhu, T. Hsiai, P.-I. Wu, R. Xiong, J. Shi, Y. Chen, Q. Zhou, and K. K. Shung, "Three dimensional printing of high dielectric capacitor using projection based stereolithography method", Nano Energy, Vol. 22, No. 2016, pp. 414-421, 2016.

[12] P. F. Jacobs, Rapid prototyping & manufacturing: fundamentals of stereolithography: Society of Manufacturing Engineers, 1992.